Clinica Chimica Acta 564 (2025) 119926

Contents lists available at ScienceDirect

Clinica Chimica Acta

journal homepage: www.elsevier.com/locate/cca

Accuracy study of Angiotensin 1–7 composite index test to predict pulmonary fibrosis and guide treatment

Nathalie De Vos [a,b,c,*], Marie Bruyneel [a,d], Alain Roman [e], Mathieu Antoine [b,c], Anne-Violette Bruyneel [f], Stephane Alard [g], Stéphanie André [a,h], Hafid Dahma [c,i], Audrey Chirumberro [d], Frédéric Cotton [a,b,j]

[a] Université Libre de Bruxelles (ULB), 50 Avenue F.D. Roosevelt, 1050 Brussels, Belgium
[b] Laboratoire Hospitalier Universitaire Bruxelles – Universitair Laboratorium Brussel (LHUB-ULB), Department of Clinical Chemistry, 322 Rue Haute, 1000 Brussels, Belgium
[c] Centre Hospitalier Universitaire (CHU) Saint-Pierre, Department of Laboratory Medicine, 322 Rue Haute, 1000 Brussels, Belgium
[d] CHU Saint-Pierre, Department of Pulmonology, 322 Rue Haute, 1000 Brussels, Belgium
[e] CHU Saint-Pierre, Department of Intensive Care Medicine, 322 Rue Haute, 1000 Brussels, Belgium
[f] Department of Physiotherapy, School of Health Sciences, HES-SO University of Applied Sciences and Arts Western Switzerland, 25 Rue des Caroubiers, 1227 Carouge, Switzerland
[g] CHU Saint-Pierre, Department of Radiology, 322 Rue Haute, 1000 Brussels, Belgium
[h] CHU Brugmann, Department of Pulmonology, 4 Place Arthur Van Gehuchten, 1020 Brussels, Belgium
[i] Laboratoire Hospitalier Universitaire Bruxelles – Universitair Laboratorium Brussel (LHUB-ULB), Department of Microbiology, 322 Rue Haute, 1000 Brussels, Belgium
[j] Hôpital Universitaire de Bruxelles (HUB), Hôpital Erasme, Department of Laboratory Medicine, 808 Route De Lennik, 1070 Anderlecht, Belgium

ARTICLE INFO

Keywords:
Respiratory Distress Syndrome
Pulmonary Fibrosis
In Vitro Diagnostic Medical Device
Precision Medicine
Interstitial Lung Diseases

ABSTRACT

Background: Pulmonary fibrosis can develop after acute respiratory distress syndrome (ARDS). The hypothesis is we are able to measure phenotypes that lie at the origin of ARDS severity and fibrosis development. The aim is an accuracy study of prognostic circulating biomarkers.
Methods: A longitudinal study followed COVID-related ARDS patients with medical imaging, pulmonary function tests and biomarker analysis, generating 444 laboratory data. Comparison to controls used non-parametrical statistics; $p < 0{\cdot}05$ was considered significant. Cut-offs were obtained through receiver operating curve. Contingency tables revealed predictive values. Odds ratio was calculated through logistic regression.
Results: Angiotensin 1–7 beneath 138 pg/mL defined Angiotensin imbalance phenotype. Hyper-inflammatory phenotype showed a composite index test above 34, based on high Angiotensin 1–7, C-Reactive Protein, Ferritin and Transforming Growth Factor-β. Analytical study showed conformity to predefined goals. Clinical performance gave a positive predictive value of 95 % (95 % confidence interval, 82 %–99 %), and a negative predictive value of 100 % (95 % confidence interval, 65 %–100 %). Those severe ARDS phenotypes represented 34 (Odds 95 % confidence interval, 3–355) times higher risk for pulmonary fibrosis development ($p < 0{\cdot}001$).
Conclusions: Angiotensin 1–7 composite index is an early and objective predictor of ARDS evolving to pulmonary fibrosis. It may guide therapeutic decisions in targeted phenotypes.

Abbreviation: ACE, Angiotensin Converting Enzyme type 1; ACE2, Angiotensin Converting Enzyme type 2; Ang-(1–7), Angiotensin 1–7; AngII, Angiotensin II; ARDS, Acute respiratory distress syndrome; AT_1R, Angiotensin II receptor type 1; AT_2R, Angiotensin II receptor type 2; AT2, Alveolar Epithelial Type II cells; AUC, Area under the curve; cAMP, cyclic Adenosine Monophosphate; CDS, Clinical decision support; CI, Confidence interval; CRP, C-Reactive Protein; COVID-19, Coronavirus disease 2019; CT, Computed tomography; ENaC, Epithelial Na+ Channel; ICU, Intensive care unit; IPF, Idiopatic pulmonary fibrosis; IQR, Interquartile range; IVD, *in vitro* diagnostic medical device; KL-6, Krebs von den Lungen 6; LDH, Lactate Dehydrogenase; MrgD, MAS-related G protein-coupled receptor, family member D; NPV, Negative predictive value; PaO_2/FIO_2, Arterial partial pressure of oxygen to fraction of inspired oxygen; PPV, Positive predictive value; PREV, Prevalence; ROC, Receiver operating curve; ROCK, RhoA and Rho-associated protein kinase; RTI, Respiratory tract infections; SARS, Severe Acute Respiratory Syndrome; SARS-CoV-2, SARS Coronavirus 2; SD, Standard deviation; SENS, Sensitivity; SPEC, Specificity; TAT, Turnaround Time; TGF-β, Transforming growth factor beta; TE, Total error; YI, Youden Index.

* Corresponding author at: LHUB-ULB, Department of Clinical Chemistry, Rue Haute 322, 1000 Brussels, Belgium.
E-mail addresses: nathalie.de.vos@ulb.be (N. De Vos), marie.bruyneel@stpierre-bru.be (M. Bruyneel), alain.roman@stpierre-bru.be (A. Roman), Mathieu.ANTOINE@LHUB-ULB.BE (M. Antoine), anne-violette.bruyneel@hesge.ch (A.-V. Bruyneel), stephane.alard@stpierre-bru.be (S. Alard), stephanie.andre@chu-brugmann.be (S. André), Hafid.DAHMA@LHUB-ULB.BE (H. Dahma), audrey.chirumberro@stpierre-bru.be (A. Chirumberro), Frederic.COTTON@LHUB-ULB.BE (F. Cotton).

https://doi.org/10.1016/j.cca.2024.119926
Received 21 June 2024; Received in revised form 12 August 2024; Accepted 13 August 2024
Available online 15 August 2024

1. Introduction

Acute respiratory distress syndrome (ARDS) and pulmonary fibrosis can develop as complications of severe respiratory tract infections (RTI), especially flagrant during pandemics. The pathophysiology of Severe Acute Respiratory Syndrome (SARS) gives insight into the fibrotic process. The hypothesis is we can measure an Angiotensin imbalance that lies at the origin of severity and pulmonary fibrosis development post-ARDS. The cellular pathway of Angiotensin is activated by the binding of SARS Coronavirus 2 (SARS-CoV-2) onto its receptor Angiotensin Converting Enzyme type 2 (ACE2) [1]. ACE2 converts Angiotensin II (AngII) into Angiotensin 1–7 (Ang-(1–7)). The heptapeptide Ang-(1–7) counter-regulates AngII. If ACE2 is unavailable and Ang-(1–7) becomes deficient, a disequilibrium occurs in favor of AngII. This causes lung damage with the production of reactive oxygen species, hypertension, vasoconstriction, an inflammatory cascade with cytokine storm, coagulopathy, and fibrosis [2,3]. Once AngII initiates the fibrotic process, a vicious circle enhances transforming growth factor beta (TGF-β), the master regulator of fibrosis [4]. Another novel biomarkers is Krebs von den Lungen 6 (KL-6), representing local damage of Alveolar Epithelial Type II cells (AT2) and AT2 hyperplasia [5,6]. The inflammation and cell injury can be measured with routinely accessible C-Reactive Protein (CRP), Ferritin, and Lactate Dehydrogenase (LDH) [7,8]. A similar approach, based on activated biological pathways and known pathogenic role, is preferred in the management of idiopatic pulmonary fibrosis (IPF) or other interstitial lung diseases [9].

The aim is to predict post-ARDS pulmonary fibrosis and guide treatment to prevent sequelae. The objectives are to study the analytical and clinical performance of novel prognostic biomarkers and more specifically Ang-(1–7) composite index test. The intended purpose of this *in vitro* diagnostics (IVD) is an easily accessible blood test for prognosis of pulmonary fibrosis and clinical decision support (CDS). The clinical role is differentiating mild RTI from severe ARDS evolving to post-ARDS pulmonary fibrosis using decisional cut-offs. Furthermore, it contributes to the practical application of a CDS for guiding treatment in specific ARDS phenotypes, aiming at preventing fibrotic sequels.

2. Materials and Methods

2.1. Study design and population

A prospective longitudinal study in respiratory medicine and critical care was designed with the following sample size, according to flowchart (Fig. 1): 567 intensive care unit (ICU) admissions for ARDS-related COVID-19 resulted in the inclusions of 87 follow-up patients after ICU-discharge. ICU hospitalized patients with positive nasal RT-PCR for SARS-CoV-2 RNA were eligible. Written informed consent was obtained from the subjects or their surrogates, according to ethical committee approval B0762020200604 (protocol number CE/20–06-04 & CE/2020/141) in CHU Saint-Pierre and CHU Brugmann institutional review board for human studies, Brussels, Belgium. The observational study was not interventional. Severe patients were randomly divided into a discovery cohort and a validation cohort. As shown in the diagram reporting the flow of participants through the study (Fig. 1), six biomarkers had been tested at 74 time points, resulting in 444 laboratory data. Remnants (500 μL) of serum, EDTA- and/or heparin-plasma were retrospectively collected at ICU. A prospective patient follow-up was done with computed tomography (CT) scan, pulmonary function tests and biomarkers at three, six and twelve months post-ICU, during pulmonology consultation between March 2020 and June 2022. The discovery cohort was collected during pandemic wave one and two, while the validation cohort encompassed wave one to four, with original wild-type SARS-CoV-2 strain and variants of interest alpha, gamma and delta. Incomplete data collections during pulmonology consultation were considered loss to follow-up and were not included. Exclusion criteria were language barrier, refusal, and psychiatric or cognitive disorders before ICU entry. The control population consisted of nineteen subjects, including nine mild or asymptomatic COVID-19 cases and ten healthy controls. The role of the control populations was to differentiate with severe ARDS-related pulmonary fibrosis patients and find decisional cut-offs. Comparison with the healthy controls gave positivity cut-offs. And comparison with the mild COVID-19 controls leaded to severity cut-offs. The statistical significant patient number was six for Ang-(1–7), based on the formula $n = [2*(1{\cdot}96 + 1{\cdot}28)2*\sigma 2]/\Delta m2$ where $\sigma = 47$ was the standard deviation and $\Delta m = 115–28 = 87$ was the difference between the biomarker mean in the pathological versus the healthy population. [10].

2.2. Test methods

Novel biomarkers were analyzed on Lumipulse® G1200 KL-6 assay (Fujirebio, Tokyo, Japan), Human Angiotensin 1–7 ELISA Kit for Research Use Only (RUO) (Novatein Biosciences, Woburn, USA and distributed by CliniScience, Brussels, Belgium) and Quantikine ELISA Human TGF-β1 Immunoassay RUO (R&D Systems, Minneapolis, USA). For KL-6 analysis, a chemiluminescent enzyme immunoassay (CLEIA) was used on Lumipulse® G1200 [11]. The CLEIA technique was based on a chemiluminescent substrate using a derivative of 1,2-dioxetane phosphate (AMPPD), to measure alkaline phosphatase as a labeling enzyme to Fab' fragments of antibody [12]. Except for radio-immunoassay [13], the method for Ang-(1–7) ELISA had not been described in literature yet. The sandwich assay described here used a 96-well microtiter plate pre-coated with monoclonal antibody specific for human Ang(1–7). The experimental protocol for Ang-(1–7) measurement followed the manufacturer's instruction BG-HUM10046: Bring kit components 20 min at room temperature, dilute rinse solution 20 times with deionized water, pipette in duplicate 50 μL of standards S1-S6 in wells, followed by 50 μL of sample diluent (considered zero standard S7)

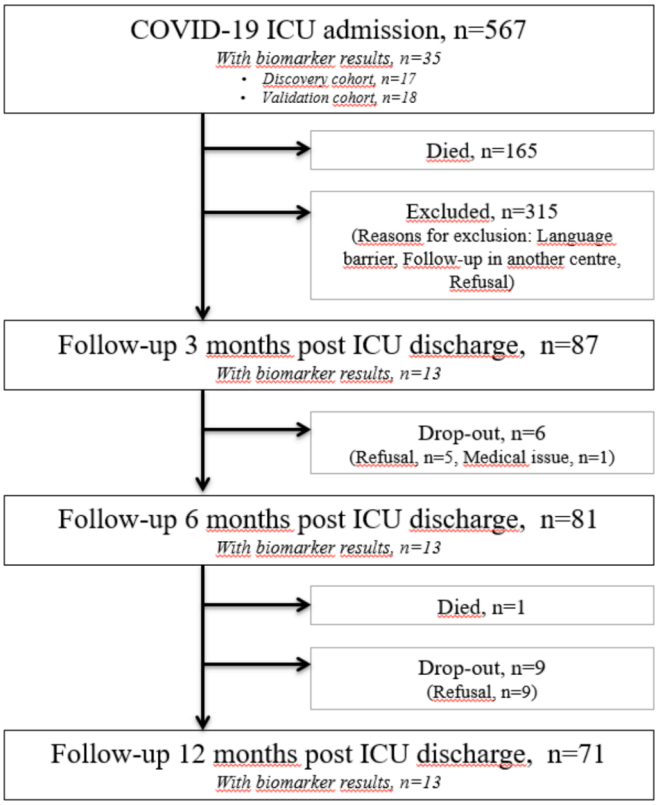

Fig. 1. Flowchart of patient population: diagram reporting the flow of participants through the study. Abbreviations: COVID-19 = Coronavirus Disease 2019, ICU=Intensive Care Unit.

and 50 μL of each patient sample, add 100 μL of red horseradish peroxidase (HRP) reagent conjugated to specific Ang-(1–7) antibody to each well, cover the microtiter plate with adhesive film, mix by tapping gently, incubate 60 min at 37 degrees Celsius, wash five times with 400 μL of wash solution per well, invert plate and hit onto absorbent paper to remove moisture between every wash step while holding strips firmly into frame, add consecutively 50 μL of chromogen solution A and B to each well containing hydrogen peroxyde and tetramethylbenzidine substrate to react with HRP, cover plate, protect from light during incubation 15 min at 37 degrees Celsius, add 50 μL stop solution of sulphuric acid, read optical density at endpoint 5 min and wavelength 450 nm with spectrophotometer and indicate S7 for blank deduction, draw a standard curve by plotting optical density on Y-axis and Ang-(1–7) concentration on X-axis, fit the curve to calculate concentration in unknown patient samples. The TGF-β1 kit had been manufactured for measuring the biologically active TGF-β1 [14], and its experimental protocol followed the manufacturer's instruction DB100B for a similar sandwich immunoassay as mentioned above.

Ferritin was tested on Cobas 8000 module c502, while CRP and LDH were measured on module c702 (Roche Diagnostics, Mannheim, Germany). Ferritin used a sandwich assay on ECLIA with Ruthenium detection method [15]. CRP was analysed with immunoturbidimetry on latex particles [16]. And LDH's catalytic activity was measured through enzymatic kinetics and ultraviolet spectrophotometric detection of reduced nicotinamide adenine dinucleotide [17].

The composite index emerged from the sum of biomarker concentrations for Ang-(1–7), CRP, Ferritin and TGF-β, divided by their respective normalization cut-off. Composite index calculation was applied on the subpopulation of high Ang-(1–7), after exclusion of patients with Ang-(1–7) deficit. The reference standard to diagnose ARDS was the Berlin Definition, based on bilateral infiltrates on chest CT and arterial partial pressure of oxygen to fraction of inspired oxygen (PaO_2/FIO_2) ≤ 300 mm Hg [18]. Pulmonary fibrosis outcome was diagnosed with CT scan.

2.3. Statistical analysis

Statistical analyses were performed using Analyse-it (Analyse-it Software, UK), GraphPad Prism 5·0 (GraphPad Software, USA) and STATA version 17·0 SE (StataCorp LLC, USA). Data were expressed as median [interquartile range (IQR)] and comparisons between groups used non-parametric tests; *p-values < 0·0500* were considered statistically significant. Additional files include mean ± standard deviation (SD). The analytical performance study encompassed trueness, precision [19], and total error (TE), beside verification of linearity. Exploratory cut-offs, fixed at the highest Youden Index (YI), and area under the curve (AUC) were analyzed using receiver operating curve (ROC) (e.g., Additional file 1 with normalization cut-offs used for composite index calculation). Sensitivity (SENS), specificity (SPEC), positive (PPV), negative predictive values (NPV) and their respective 95 % confidence intervals (CI) were calculated with contingency tables and Wilson formula in the clinical performance study. Any potential sources of bias were addressed through age randomization in discovery versus validation cohort and gender stratification. Odds ratios were calculated through bivariate logistic regression (Additional file 2).

3. Results

3.1. Demographic and clinical characteristics

Baseline demographic and clinical patient characteristics at ICU were 63 % female survivors, mean age of 57 ± 12 years, 55 % obese, 56 % arterial hypertension, 45 % diabetes, a hospital length of stay of 29 ± 18 days and 18 ± 14 days at ICU, 51 % with mechanical ventilation and 8 % extracorporeal membrane oxygenation [20]. All severe patients had ARDS at ICU. And 85 % evolved to pulmonary fibrosis sequelae on CT scan during the first year post-ICU, with 9 ± 7 affected lung segments, leading to impaired diffusing capacity of the lungs for carbon monoxide (DLCO) < 80 % in 44 % of patients [20–22]. Within the population of post-ARDS pulmonary fibrosis, there was a significantly lower prevalence (PREV) in patients with less affected segments (<6), compared to many affected segments (6–20) on chest CT scan, showing respectively PREV=37 % versus 63 % (*p < 0·0500*). At one year post-ICU, 23 % had decreased total lung capacity and 18 % decreased forced expiratory volume one < 80 % [20]. Preliminary data at 2 years of follow-up, resulted in PREV=55 % for post-ARDS pulmonary fibrosis. Radiological data shown in additional file 3, illustrated the follow-up of CT sequelae with ground-glass opacities in one patient, evolving from COVID-19-induced ARDS to pulmonary fibrosis. Mild or asymptomatic COVID-19 patients were 40 % female, 49 ± 15 years old, and had a favorable outcome without respiratory sequelae.

3.2. Analytical performance and biomarker profiles

The analytical performance study demonstrated conformity to predefined acceptance criteria for all novel biomarkers (Table 1): Ang-(1–7) showed TE < 37·7%, TGF-beta gave TE < 33·3% and KL-6 stayed within TE < 20·8%. Matrix comparison yielded no statistical difference between heparin plasma and serum for Ang-(1–7) and KL-6 *(p > 0·0500)*, but significant difference for TGF-β *(p < 0·0017)*. Although EDTA-plasma was possible for Ang-(1–7), it was contra-indicated for TGF-β because of platelet preservation and interference by degranulation.

Biomarker profiles were realized on patient samples at ICU and in follow-up post-ICU. At ICU, the severe COVID-19 patients showed

Table 1
Analytical performance specifications for novel biomarkers.

		Ang-(1–7)	TGF-β	KL-6
Performance at given concentration		250 pg/mL	612 pg/mL	330 U/mL
	Trueness (bias)	1.5 % *	11.4 % **	7.9 % ***
	Precision, repeatability (CV_{intra})	6.7 % *	1.8 % **	6.1 %
	Precision, reproducibility (CV_{inter})	14.5 % *	9.5 %	7.2 %
	Total Error (TE)	25.4 % *	27.1 % **	19.6 % ***
Measuring range		16–500 pg/mL	31–2000 pg/mL	50–10000 U/mL
Linearity				
	Range	63–500 pg/mL	63–2000 pg/mL	26–816 U/mL
	Simple linear regression	y = 0.9065x-7.1416	y = 1.0163x + 24.978	y = 0.9966x-21.298
	Correlation coefficient	R^2 = 0.998	R^2 = 0.996	R^2 = 0.995

Biological variation from European Federation of Clinical Chemistry and Laboratory Medicine (EFLM) and Westgard Ricos Biological Variation Database (Westgard) were used to obtain desirable analytical performance specifications from related biomarkers.
Abbreviations: Ang-(1–7) = Angiotensin 1–7, TGF-β = Transforming Growth Factor beta, KL-6 = Krebs von den Lungen 6, CV_{intra} = intra-run coefficient of variation, CV_{inter} = inter-run coefficient of variation, TE=total error = bias+(1,65*CV_{inter}).
* conform to EFLM for renin, because Ang-(1–7) is physiologically related to Renin-Angiotensin-Aldosterone System (bias = 12.8 %, CV=15.1 %, TE=37.7 %).
** conform to Westgard for Collagen type III N Propeptide (PIIINP), because TGF-β influences collagen formation in the extracellular matrix (bias = 22.1 %, CV=6.8 %, TE=33.3 %),
*** conform to EFLM for CA15.3, because of structural homology to KL-6 within mucin1 family (bias = 15.8 %, CV=3.1 %, TE=20.9 %).

significantly higher Ang-(1–7), TGF-β, KL-6, CRP, Ferritin and LDH compared to healthy controls *(p < 0·0500)*. Expected values in normal and pathological populations were calculated (Additional file 4). Severe patients with ARDS at ICU showed Ang-(1–7) deficit of 124 [81–154] pg/mL in early stages of acute SARS infection, and this was significantly lower compared to mild coronavirus patients with Ang-(1–7) = 147 [138–201] pg/mL *(p < 0·0500)* (Fig. 2).

Three months after ICU, Ang-(1–7) normalized below its cut-off of < 57 pg/mL and did not show any alteration up to twelve months of follow-up. After ICU-discharge, CRP, Ferritin and LDH returned normal in 90 % of severe coronavirus patients, with their respective cut-offs at < 5 mg/L, < 62 μg/L and < 182 U/L. After one year, KL-6 (cut-off < 275 U/mL) and TGF- β (cut-off < 34968 pg/mL) normalized in only 25 %, respectively 33 % of severe COVID-19 patients. Within the first year of follow-up post-ICU, the mean KL-6 value in the patient population did not significantly change at different measuring moments *(p = 0·6333)* (Additional file 5), while TGF-β decreased gradually at three, six and twelve months post-ICU *(p < 0·0001)* (Additional file 6).

3.3. Clinical performance

The clinical performance study resulted in cut-offs for differentiating mild coronavirus controls from severe ARDS patients with pulmonary fibrosis sequels. Two severe ARDS phenotypes were characterized using consecutive diagnostic steps. The first step concerned the diagnosis of Ang-(1–7) deficit = 107 [48–123] pg/mL. The cut-off to determine Ang-(1–7) deficit was < 138 pg/mL in the discovery cohort, with SENS=65 % (95 %CI, 41 %–83 %), SPEC=86 % (95 %CI, 49 %–97 %), PPV=92 % (95 %CI, 65 %–99 %), NPV=50 % (95 %CI, 25 %–75 %). To resolve the resulting overlap of populations and select the best AUC, a combination of relevant biomarkers was proposed in a second step, using the calculation of a composite index test combining indices of high Ang-(1–7), Ferritin, CRP and TGF-β. When the composite index was analyzed within the subpopulation of preliminary high Ang-(1–7) (Fig. 3), we obtained strong statistical power to differentiate two distinct populations *(p = 0·0173)*: the severe/critical patients (hyper-inflammatory phenotype) showed a median composite index of 42 [36-55] and the mild/asymptomatic (hypo-inflammatory phenotype) had a median composite index of 13 [10-36].

In the discovery cohort, the composite index showed a cut-off of > 34 to predict a more severe COVID-19 at ICU and evolution to post-ARDS pulmonary fibrosis, with PPV=83 % (95 %CI, 44 %–97 %), NPV=80 % (95 %CI, 38 %–96 %), SENS=83 % (95 %CI, 44 %–97 %), SPEC=80 % (95 %CI, 38 %–96 %), at YI=0·800, AUC=0·933. The AUC of 0·933 from the Ang-(1–7) composite index test was higher than the AUC from individual biomarkers, each below or equal to 0·800 (Table 2).

3.4. Clinical decision support

The above-mentioned IVD tests were linked to therapeutic decisions through a CDS (Fig. 4).

In step one, on the left side of the algorithm, patients with an Ang-(1–7) deficit (<138 pg/mL) were eligible for substitution therapy with Ang-(1–7) agonists and novel expensive therapies beside standard of care; these patients represented the phenotype of Angiotensin imbalance. In step two, a composite index was calculated using high Ang-(1–7), Ferritin, CRP and TGF-β. Indeed, the subpopulation of high Ang-(1–7) patients (=155 [153–173] pg/mL), were analyzed with a composite index test to enhance statistical power and distinction with mild COVID-19 showing Ang-(1–7) of 147 [138–201] pg/mL. At the middle of the CDS, the patients with high composite index > 34 represented the hyper-inflammatory phenotype. They could benefit from protective treatments beside standard of care, but would not be eligible for Ang-(1–7) agonists. On the right side of the CDS, the patients with low composite index ≤ 34 represented the hypo-inflammatory phenotype with low risk for developing pulmonary sequelae. For the hypo-

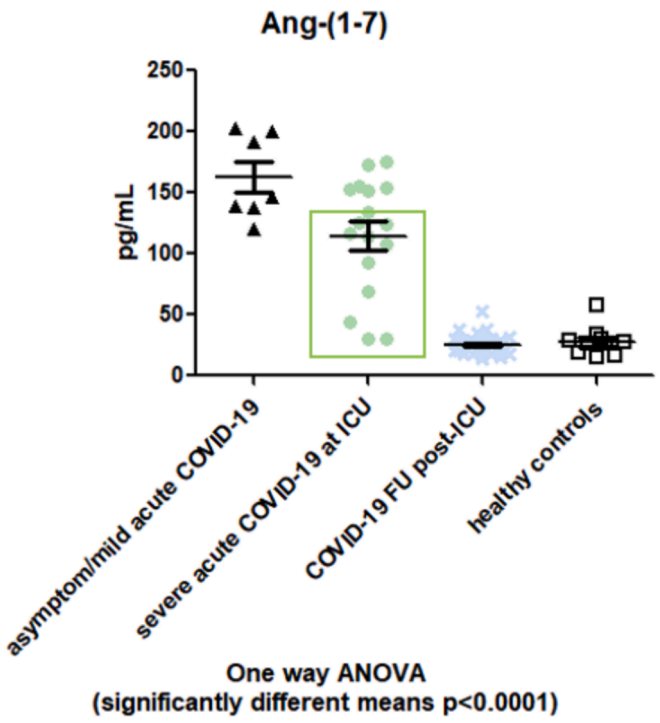

Fig. 2. Ang-(1–7) in severe COVID-19 patients at ICU and follow-up post-ICU during the first year, compared to asymptomatic/mild COVID-19 and healthy controls. Green box: Angiotensin imbalance phenotype. Abbreviations: Ang-(1–7) = Angiotensin 1–7, ICU=Intensive Care Unit, FU=follow-up.

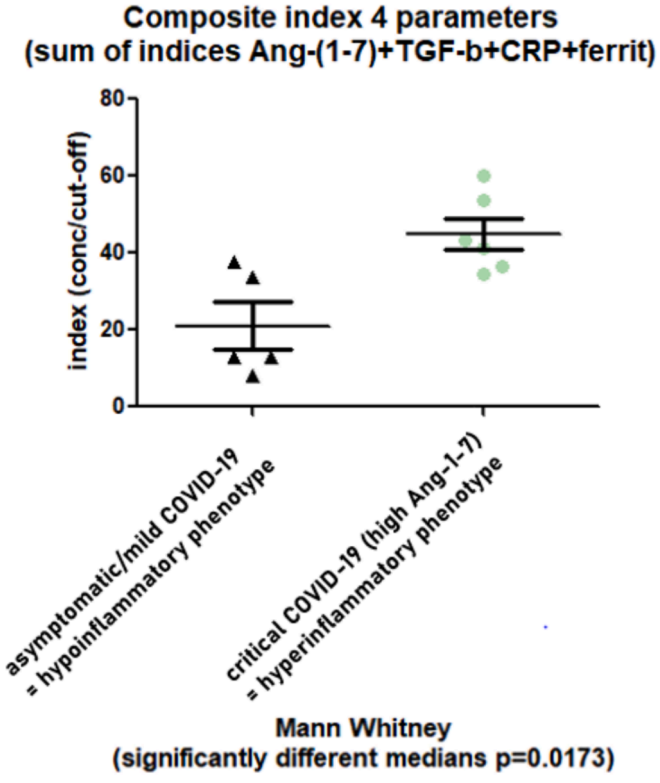

Fig. 3. Mann-Whitney of the composite index test based on high Ang-(1–7), TGF- β, CRP and Ferritin. Abbreviations: Ang-(1–7) = Angiotensin 1–7, TGF-β = Transforming Growth Factor beta, CRP=C-Reactive Protein, conc/cut-off = the concentration of each biomarker is divided by its cut-off to obtain a biomarker index, composite index = sum of all biomarker indices.

Table 2
AUC for different tested models.

	AUC	Severity cut-off
Individual biomarker		
Ang-(1–7)	0·773	< 138 pg/mL
CRP	0·744	> 47 mg/L
Ferritin	0·589	> 487 µg/L
TGF-β	0·750	> 47008 pg/mL
LDH	0·800	> 338 IU/mL
KL-6	0·714	> 422 U/mL
4-Parameter composite index	0·933	> 34
3-Parameter composite index	0·933	> 33

AUC was based on ROC for differentiating severe ARDS-related pulmonary fibrosis patients from mild COVID-19 controls. Abbreviations: AUC=Area Under the Curve, ROC=Receiver Operating Curve, Ang-(1–7) = Angiotensin 1–7, CRP=C-reactive Protein, TGF-β = Transforming Growth Factor beta, LDH=Lactate Dehydrogenase, KL-6 = Krebs von den Lungen 6, 4-Parameter composite index = sum of individual indices of high Ang-(1–7) + Ferritin + CRP+TGF-β, 3-Parameter composite index = sum of individual indices of high Ang-(1–7) + Ferritin + CRP.

inflammatory phenotype, the therapeutic approach could possibly be limited to standard of care. All treatment decisions would be made according to the full clinical context, anamnesis, medical history, pulmonary function tests, medical imaging and international guidelines. CDS resulted in three prognostic biomarker profiles or phenotypes, as recapitulated in Table 3. The Angiotensin imbalance and hyper-inflammatory phenotypes were considered severe phenotypes with a risk for sequelae. ARDS was significantly associated with severe phenotypes ($p < 0{\cdot}001$). At 3 months post-ICU, there was also an association between the severe phenotypes and pulmonary fibrosis ($p < 0{\cdot}001$). Patients with severe phenotypes had 76 (Odds ratio 95 %CI, 6–962) times more risk for ARDS, and 34 (Odds ratio 95 %CI, 3–355) times more risk of developing pulmonary fibrosis.

The three phenotypes were subsequently validated with a bicentric validation cohort. Thirteen patients fell within the Angiotensin imbalance phenotype, five were characterized hyper-inflammatory and four hypo-inflammatory; the mortality rate was 31 %, 20 %, and 0 %, respectively. A cross tabulation comprised the full discovery plus validation cohort with PPV=95 % (95 %CI, 82 %–99 %) and NPV=100 % (95 %CI, 65 %–100 %), beside stratification per gender (Additional file 7). In addition, the existence of an Angiotensin imbalance phenotype was replicated in an independent international validation cohort (preliminary data not shown). Downwards the CDS, during the follow-up period post-ARDS, positive TGF-β > 34968 pg/mL and/or KL-6 > 275 U/mL in association with clinical and radiological impairment, could indicate eligibility for antifibrotic treatments.

As multiple biomarkers were tested, multiple statistical testing had been adjusted (cfr. Additional file 8). Beside the four-parameter composite index, statistics functioned with a three-parameter (without TGF-β) or a five-parameter composite index (with LDH) ($p < 0{\cdot}0500$). With

Table 3
Characteristics of three phenotypes with prognostic biomarker profiles in SARS.

Phenotype	Ang-(1–7)	4-Parameter composite index	Severity	Sequelae
Angiotensin imbalance	< 138 pg/mL	NA	severe or critical	yes
Hyper-inflammatory	≥ 138 pg/mL	> 34	severe or critical	yes
Hypo-inflammatory	≥ 138 pg/mL	≤ 34	mild or asymptomatic	no

Abbreviations: Ang-(1–7) = Angiotensin 1–7, 4-Parameter composite index = sum of individual indices of Ang-(1–7) + Ferritin + CRP+TGF-β, NA=not applicable, Sequelae = post-ARDS pulmonary fibrosis.

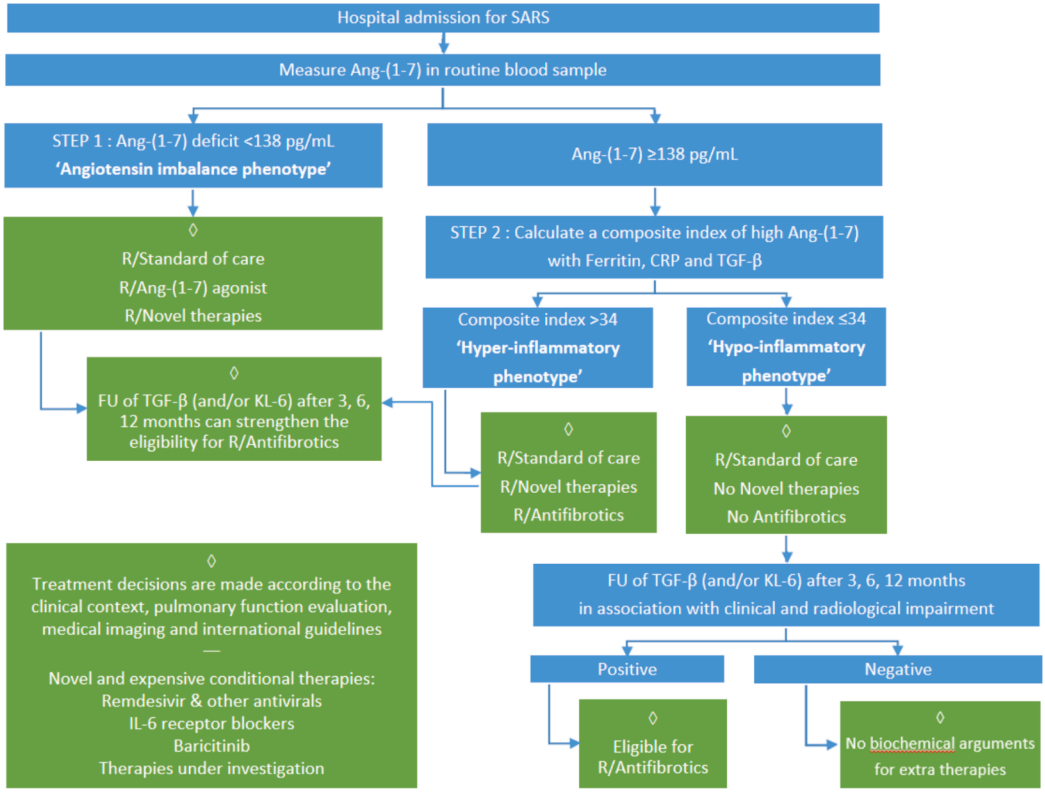

Fig. 4. Clinical decision support for ARDS phenotypes. Abbreviations: ARDS=Acute Respiratory Distress Syndrome, SARS=Severe Acute Respiratory Syndrome-–associated coronavirus, Ang-(1–7) = Angiotensin 1–7, CRP=C-Reactive Protein, TGF-β = Transforming Growth Factor beta, KL-6 = Krebs von den Lungen 6, FU=Follow-up, R/=Recipe = option for administration.

KL-6, statistical significance was lost ($p = 0{\cdot}1429$). At least, high Ang-(1–7), Ferritin, and CRP were mandatory for the three-parameter composite index; the cut-off was placed at > 33 (YI=0·800, AUC=0·933) and gave PPV=83 % (95 %CI, 44 %–97 %), NPV=80 % (95 %CI, 38 %–96 %), SENS=83 % (95 %CI, 44 %–97 %), and SPEC=80 % (95 %CI, 38 %–96 %). Without the distinction of Ang-(1–7) deficit in step one, the composite index could not be used ($p = 0{\cdot}2684$).

4. Discussion

4.1. Key Results

Ang-(1–7) and its composite index test are early and objective predictors of severity and post-ARDS pulmonary fibrosis. Accuracy study shows conformity to analytical and clinical goals, with PPV of 95 % (95 %CI, 82 %–99 %) and NPV of 100 % (95 %CI, 65 %–100 %). An ARDS patient belonging to the Angiotensin imbalance or hyper-inflammatory phenotype has 34 (Odds ratio 95 %CI, 3–355) times more risk for developing pulmonary fibrosis. A CDS guides therapeutic decisions in targeted ARDS phenotypes, aiming at preventing severity and sequelae. The utility lies in ready-to-use biomarkers as an add-on to routine sample collection at hospital admission, for objective prediction of pulmonary fibrosis sequels, to rely rapidly on focused treatment. In addition, it can help in triage at hospital entry for ICU referral, when the patient is stratified as “high risk” for ARDS and pulmonary fibrosis development.

4.2. Interpretation

We observe three distinct phenotypical behaviors in the acute setting, which guide physicians in targeting the right therapy for the right patient: the Angiotensin imbalance (Ang-(1–7) < 138 pg/mL), the hyper-inflammatory (composite index > 34) and the hypo-inflammatory phenotypes. This study is yet another indication of the existence of ARDS subphenotypes, which is a promising stratification tool for precision medicine [23–27]. Indeed, a focused therapeutic choice can be made before the sequels develop. The CDS limits expensive novel therapies to targeted patient subpopulations, supports healthcare economy and prevents eventual side effects. Furthermore, this CDS enables prospective patient stratification in clinical trials to obtain treatment efficacy. Emerging drug candidates in post-ARDS pulmonary fibrosis are listed in Additional file 9. Ang-(1–7) supplementation therapy is under investigation in clinical trials and its administration should be limited to Angiotensin imbalance phenotype [28]. We do not expect treatment efficacy of Ang-(1–7) agonists in the hyper-inflammatory phenotype. Objective biochemical arguments exist in the hyper-inflammatory phenotype to receive other novel therapies beside standard of care. Those high-risk groups are also eligible for antifibrotics, depending on clinical trials and in function of TGF-β and/or KL-6 levels during follow-up. Whether TGF-β and KL-6 can monitor the response to therapy over time, needs to be further investigated. Treatment can be limited in the hypo-inflammatory phenotype, because of better clinical outcome, as described in literature [23].

Biomarker profiling elucidates the pathophysiology and determines the indication of each biomarker. Ang-(1–7) plays a prognostic role in early SARS and ARDS at hospital admission. Mild or asymptomatic coronavirus shows activated Angiotensin pathway through high concentrations of Ang-(1–7), representing an equilibrium between pulmoprotective Ang-(1–7) and pulmodestructive AngII. On the contrary, Ang-(1–7) deficit corresponds to dysregulation of the physiological homeostatis, leading to deleterious effects caused by AngII [4]. As such, Angiotensin imbalance explains the pathogenesis of severe coronavirus and pulmonary fibrosis. The mechanism behind Ang-(1–7) deficit is decreased availability of ACE2 and insufficient degradation of AngII. ACE2 availability is hindered by SARS binding, ACE2-cleavage, viral cytopathic effect on AT2 and ACE2-downregulation during subsequent AT2 hyperplasia [4]. Surprisingly, a double Ang-(1–7) population is found in severe COVID-19, one with Ang-(1–7) deficit (the Angiotensin imbalance phenotype) and another without Ang-(1–7) deficit but with remarkable inflammation (the hyper-inflammatory phenotype). In the latter, we speculate that enough Ang-(1–7) product is metabolized thanks to shedding of active ACE2 or alternative enzymatic actions, like prolyloligopeptidase, neprilysin or thimet oligopeptidase [1]. The hyper-inflammatory phenotype shows increased composite index test with high Ang-(1–7), CRP, Ferritin, and TGF- β. Ferritin is liberated from activated macrophages and TGF- β signals emanate from macrophages [29]. The pathophysiologic cascade of TGF-β is triggered by the SARS-CoV-2 entry into the alveolar epithelial cells and plays a role in ARDS [30], which further induces lung fibrosis [4]. Indeed, TGF-β modulates pulmonary fibrosis by recruiting monocytes/macrophages, differentiating fibroblasts, inducing extracellular matrix synthesis and pathologic airway remodeling. After ICU, Ang-(1–7), CRP, Ferritin, and LDH normalize. This corroborates findings of a British cohort during follow-up for Long COVID [31]. Interesting biomarkers for follow-up are TGF-β and KL-6, because they have been linked to pulmonary fibrosis and they persist during at least one year after ICU [32–34]. TGF-β knows gradual decrease over time while high KL-6 stagnates. Improvement of TGF-β may be linked to clinical recovery. Indeed, post-COVID pulmonary fibrosis seems to show better pulmonary function than usually seen in IPF, despite equal degrees of radiological involvement [35]. Moreover, the radiological image correlates with KL-6, especially the extent of affected segments on CT scan [36,37]. Further examination will correlate TGF-β, KL-6, clinical and radiological findings up to two years after ICU discharge. Clinical monitoring at regular intervals is state of the art for IPF [38]. Similarly, monitoring could be considered for post-ARDS pulmonary fibrosis, possibly even expanded with biomarker dosages for TGF-β and KL-6.

The diagnosis of an Ang-(1–7) deficit precedes the calculation of the composite index, composed of minimum three parameters (high Ang-(1–7), CRP, Ferritin); the association of TGF- β or LDH is facultative. Nevertheless, the panel used in this four-parameter composite index has a strong AUC of 0·933. The selected biomarkers Ang-(1–7), CRP, Ferritin and TGF- β reflect a combination of distinct biological pathways, having their pathogenic role in ARDS and pulmonary fibrosis. The Ang-(1–7) imbalance relates to acute lung injury at the alveolo-capillary interface and initiates fibrosis, while TGF- β maintains the fibrotic process. CRP and Ferritin represent the inflammatory cascade. They have been selected out of a broad COVID-19 biochemistry panel [7,39]. The multi-organ dysfunction parameters with insufficient statistical power (data not shown), have not been retained: procalcitonin, cardiac troponin, creatinine, transferrin, iron, and Angiotensin Converting Enzyme type 1 (ACE) with direct enzyme activity measurement. Still, the interest remains for a genetic measurement of ACE polymorphism in the context of COVID-19 epidemiology [40].

The data of our study have been found in an ARDS-related COVID-19 population. Post-acute sequelae, including post-ARDS pulmonary fibrosis, represent a focus of research since the coronavirus pandemic [29]. The global PREV of ARDS in COVID-19 patients is 32 %; around half of them survive (23–56 %) [41]. Our findings confirm that ARDS survivors develop pulmonary fibrosis more frequently if many segments are affected on chest CT scan [42]. The higher PREV found during the first year of follow-up, can be explained by the strength of our study, with a clearly stratified severely affected patient population at ICU, supported by serious radiological lesions. At 2 years, our preliminary data show PREV=55 % for post-ARDS pulmonary fibrosis. PREV of persistent fibrotic lesions after COVID-19 is estimated 11–75 % in literature, and varies considerably according to differences in study design, methodology, patient population, severity of illness, timing of assessment, follow-up duration, vaccination status, and geographical region [42–44].

The intended purpose has been met, and the clinical use has a double relevance; on the one hand during SARS resurgence, and on the other

hand, it opens perspectives on applying this diagnostic approach to ARDS from other etiologies, outside the scope of COVID-19. Indeed, it will be interesting to investigate the CDS in different ARDS etiologies like bacterial pneumonia, aspiration, trauma, and viral RTI, like severe influenza, because of comparable respiratory failure [45]. Whether COVID-related ARDS may be generalizable to other forms of ARDS, is under investigation in a broader international cohort and preliminary data are promising.

Both the signaling pathways of Ang-(1–7) and TGF-β play a theoretical role in ARDS from all etiologies, including but not restricted to COVID-19. [30] Initially, endothelial injury is caused by inflammatory events, which is noticeable by high CRP and Ferritin concentrations. According to *in vitro* and *in vivo* models, injured endothelium impacts ACE and ACE2 activity, leading to Angiotensin imbalance. [46] Angiotensin imbalance in favor of Ang II activates the cytoskeleton rearrangement in pulmonary vascular endothelial cells through RhoA and Rho-associated protein kinase (ROCK), causing vessel hyperpermeability and alveolar-capillary barrier dysfunction. [30,46] This contributes to the typical alveolar edema in ARDS and ventilation-perfusion mismatch, which enhance hypoxia and hypercapnia. Hypoxia and/or hypercapnia upregulates the activity of Ang II and Ang-(1–7), and might alter the balance between both. [47] Ang II mediates pulmonary vasoconstriction, hypertension and microvascular hypoxia, while Ang-(1–7) mediates vasodilation via Angiotensin II receptor type 2 (AT_2R). [48] Furthermore, when Ang II binds Angiotensin II receptor type 1 (AT_1R) onto alveolar epithelial cells, it inhibits cyclic adenosine monophosphate (cAMP). In turn, the inhibited cAMP decreases epithelial Na^+ channel (ENaC) expression and impairs alveolar fluid clearance. [46] On the contrary, cAMP is produced upon Ang-(1–7) binding onto MAS-receptor or MrgD-receptor. [48] One might suppose that this molecular Ang-(1–7) action on cAMP could increase ENaC expression and clear alveolar fluid, but *in vivo* studies are warranted.

TGF-β decreases ENaC expression, through canonical Small mothers against decapentaplegic (Smad) signaling, therefore impairing alveolar fluid clearance. [46] Furthermore, TGF-β/Smad signaling triggers profibrotic gene overexpression through the main cytoplasmic downstream regulators Smad2 and Smad3. [30,49] In a Smad-independent pathway, TGF-β activates Nuclear factor-kappa B (NF-κB). NF-κB is another key signal transduction pathway in endothelial cell dysfunction in ARDS. [50] While NF-κB is induced by Ang II onto its receptor AT_1R [48], NF-κB is suppressed by Ang-(1–7) onto its MAS-receptor. [51] NF-κB leads to the transcription of inflammatory genes, macrophage recruitment and cytokine storm. It maintains inflammation through activation of fibroblasts. NF-κB renders the endothelium permissive for massive infiltration of polymorphonuclear leukocytes. [50] Besides, NF-κB can downregulate the anticoagulation proteins to cause intravascular coagulation. [30].

During ARDS progression, alveolar edema is reinforced through inflammatory injury towards the alveolar epithelium, causing cell death and subsequent epithelial cell hyperplasia. A pivotal phenomenon is the epithelial-mesenchymal transition, which comes along with the expression of profibrotic proteins, and ultimately induces pulmonary fibrosis. [30] Whether this process of AT2 injury and remodeling continuously releases KL-6, remains hypothetic. Although the role of KL-6 in the pathophysiology has still to be elucidated, increased levels of KL-6 have been reported both in COVID-related ARDS and ARDS from other etiologies [52], as well as in pulmonary fibrosis.

Oxidative stress is a stimulus for epithelial cell death and for NF-κB activation. [50] The oxidative stress induced by Ang II/AT_1R can be counter-balanced by Ang-(1–7)/MAS through ROCK inhibition. [53] This way, Ang-(1–7) protects against lung fibroblast migration and lung fibrosis in *in vitro* and *in vivo* models. Another supposed benefit of ROCK inhibition thanks to Ang-(1–7) increase, would be the cytoskeleton reorganization and the restoration of the alveolar-capillary membrane integrity, representing an interesting research field. An additional advantage of Ang-(1–7) is its anti-inflammatory effect. [48].

Following from the above-mentioned underlying cellular signal transduction mechanisms, Ang-(1–7) concentration and composite index might play a role in phenotyping ARDS and ARDS-related pulmonary fibrosis from undetermined etiologies in the future, whereby SARS among other viruses or common causes may lie at the origin.

The strength of this study is the population characterization with demographic, biochemical, radiological, and clinical data, including pulmonary function tests.

4.3. Limitations

Although the Odds ratio for pulmonary fibrosis in severe SARS shows a wide 95 % CI (3–335), the lowest range of the CI still reveals statistical significance. Despite wide CI, this study conceptualizes an evolution from a pulmoprotective Ang-(1–7) situation to a pulmodestructive Ang II. The calculation for statistical significant patient number applies to the proposed cut-offs; it does not offer the possibility to draw strong conclusions considering clinical endpoints. Concerning matrix limitations, the routine serum tube or heparin plasma could be used for Ang-(1–7) concentration and the 3-parameter composite index, while serum is the dedicated matrix for TGF-β and the 4-parameter composite index.

CDS can be integrated in digital health, but cannot replace the complete medical context. Even if prescribers have easy access to the circulatory biomarkers depicted in this study, because of direct applicability in routine core laboratories, a large-scale assay for Ang-(1–7) should be developed on an automatic analyzer, for faster diagnostics at a lower cost. The cost for the RUO test is €53 for Ang-(1–7) and €105 for TGF-β per patient sample including the manipulation by an experienced lab technician, while working in batch with a turnaround time (TAT) of one week. TGF-β RUO manipulation includes preparative steps for sample activation. Cost and TAT can be estimated for clinical use in a routine hospital lab. On an auto-analyzer with a short hands-on time, the great advantage would be a TAT of 2 h and 24/7 availability. Although it is not yet possible to fix the price per test, it would probably vary between €20 and €40.

Another limitation is the lack of golden standard for Ang-(1–7) measurement, so concentrations from different studies are not comparable. Previous publications report a single Ang-(1–7) population, while our study shows for the first time a double Ang-(1–7) population. This may partly explain the contradictions in literature on increased versus decreased Ang-(1–7) [54,55]. Complete sample collection is a difficulty at different time points, due to patient drop-out. Therefore, a larger international validation with independent ARDS patients is ongoing to strengthen our findings. Because the discovery cohort only contained survivors during follow-up after ICU, and because of the limited number of patients in the validation cohort, data on mortality are not robust enough to draw conclusions.

5. Conclusions

The prognostic biomarkers for post-ARDS pulmonary fibrosis decrypted in this study, offer a promising personalized approach through specific ARDS phenotypes and may facilitate targeted therapies to limit sequelae. Ang-(1–7) composite index represents a triggered pathway playing a central role in dysregulated lung repair and the fibrotic process, enhanced by TGF-β through a vicious circle. The relevance of using this IVD in routine, is to objectively predict ARDS severity and pulmonary fibrosis sequelae, on an easy blood collection at hospital entry, early in the clinical decision process.

CRediT authorship contribution statement

Nathalie De Vos: Conceptualization, Data curation, Formal analysis, Funding acquisition, Investigation, Methodology, Project administration, Resources, Software, Validation, Visualization, Writing – original draft, Writing – review & editing. **Marie Bruyneel:** Writing – review &

editing, Validation, Supervision, Resources, Project administration, Methodology, Investigation, Data curation, Conceptualization. **Alain Roman:** Writing – review & editing, Validation, Supervision, Resources, Project administration. **Mathieu Antoine:** Writing – review & editing, Resources, Data curation. **Anne-Violette Bruyneel:** Writing – review & editing, Software, Resources, Formal analysis, Data curation. **Stephane Alard:** Writing – review & editing, Validation, Resources, Data curation. **Stéphanie André:** Writing – review & editing, Resources, Data curation. **Hafid Dahma:** Writing – review & editing, Resources, Data curation. **Audrey Chirumberro:** Writing – review & editing, Resources, Data curation. **Frédéric Cotton:** Writing – review & editing, Validation, Supervision, Resources, Methodology, Investigation, Conceptualization.

Declaration of competing interest

The authors declare that they have no known competing financial interests or personal relationships that could have appeared to influence the work reported in this paper. NDV and FC declare International Patent PCT/EP2023/051954 - WIPO WO2023144281A1 (European Patent Office EP22153733.5).

Data availability

Data will be made available on request.

Acknowledgements

We gratefully thank Philippe de Diesbach, Frédéric Pierard, Eldar Smajic and Marc Bertrand-Enche for their insights.

Funding

Reagents were funded by LHUB-ULB, Laboratoire Hospitalier Universitaire Bruxelles – Universitair Laboratorium Brussel, Belgium.

Ethics approval and consent to participate

Written informed consent was obtained from the subjects or their surrogates, according to ethical committee approval B0762020200604 (protocol number CE/20-06-04 & CE/2020/141) in CHU Saint-Pierre and CHU Brugmann institutional review board for human studies, Brussels, Belgium.

Consent for publication

Consent to participate and publish was acquired from each patient/participant. The ethical conduct of research involving human subjects complies with the World Medical Association Declaration of Helsinki.

Authors' contributions

Data collection : NDV, MB, AR, MA, SAL, SAN, HD, AC. Conceptualization : NDV, FC, MB. Data curation : NDV, MB, AVB, MA, SAL, SAN, HD, AC. Statistics and formal analysis : NDV, AVB. Funding acquisition : NDV. Investigation and data interpretation : NDV, MB, FC. Methodology : NDV, FC, MB. Project administration : NDV, MB, AR. Resources : NDV, MB, AR, MA, AVB, SAL, SAN, HD, AC, FC. Supervision : FC, MB, AR. Software : NDV, AVB. Validation : NDV, FC, MB, AR. Visualization : NDV, SAL. Writing – original draft : NDV. Writing – review & editing : NDV, MB, AR, MA, AVB, SAL, SAN, HD, AC, FC. All authors contributed to critical revision of the manuscript and provided final approval for the version to be published. Literature search : NDV, MB.

Appendix A. Supplementary material

Supplementary data to this article can be found online at https://doi.org/10.1016/j.cca.2024.119926.

References

[1] F. Pucci, F. Annoni, R.A.S. dos Santos, F.S. Taccone, M. Rooman, Quantifying renin-angiotensin-system alterations in covid-19, Cells 10 (2021) 2755, https://doi.org/10.3390/cells10102755.

[2] F. Silhol, G. Sarlon, J.C. Deharo, B. Vaïsse, Downregulation of ACE2 induces overstimulation of the renin–angiotensin system in COVID-19: should we block the renin–angiotensin system? Hypertens. Res. 43 (2020) 854–856, https://doi.org/10.1038/s41440-020-0476-3.

[3] B.M. Henry, J. Vikse, S. Benoit, E.J. Favaloro, G. Lippi, Hyperinflammation and derangement of renin-angiotensin-aldosterone system in COVID-19: A novel hypothesis for clinically suspected hypercoagulopathy and microvascular immunothrombosis, Clin. Chim. Acta 507 (2020) 167–173, https://doi.org/10.1016/j.cca.2020.04.027.

[4] M.V. Delpino, J. Quarleri, SARS-CoV-2 Pathogenesis: Imbalance in the Renin-Angiotensin System Favors Lung Fibrosis, Front. Cell. Infect. Microbiol. 10 (2020) 340, https://doi.org/10.3389/fcimb.2020.00340.

[5] P. Lavis, S. Morra, C. Orte Cano, N. Albayrak, V. Corbière, V. Olislagers, N. Dauby, V. del Marmol, A. Marchant, C. Decaestecker, F. Mascart, N. De Vos, P. van de Borne, I. Salmon, M. Remmelink, M. Parmentier, A.K. Cardozo, B. Bondue, Chemerin plasma levels are increased in COVID-19 patients and are an independent risk factor of mortality, Front. Immunol. 13 (2022) 941663, https://doi.org/10.3389/fimmu.2022.941663.

[6] M. d'Alessandro, P. Cameli, R.M. Refini, L. Bergantini, V. Alonzi, N. Lanzarone, D. Bennett, G.D. Rana, F. Montagnani, S. Scolletta, F. Franchi, B. Frediani, S. Valente, M.A. Mazzei, F. Bonella, E. Bargagli, Serum KL-6 concentrations as a novel biomarker of severe COVID-19, J. Med. Virol. 92 (2020) 2216–2220, https://doi.org/10.1002/jmv.26087.

[7] C. Skevaki, P.C. Fragkou, C. Cheng, M. Xie, H. Renz, Laboratory characteristics of patients infected with the novel SARS-CoV-2 virus, J. Infect. 81 (2020) 205–212, https://doi.org/10.1016/j.jinf.2020.06.039.

[8] B. M. Henry, M. H. S. de Oliveira, S. Benoit, M. Plebani, G. Lippi, Hematologic, biochemical and immune biomarker abnormalities associated with severe illness and mortality in coronavirus disease 2019 (COVID-19): A meta-analysis, Clin. Chem. Lab. Med. 58 (2020) 1021-1028. Doi: 10.1515/cclm-2020-0369.

[9] G.Y. Liu, G.R.S. Budinger, J.E. Dematte, Advances in the management of idiopathic pulmonary fibrosis and progressive pulmonary fibrosis, BMJ 377 (2022) e066354.

[10] X. Wang, X. Ji, Sample Size Estimation in Clinical Research: From Randomized Controlled Trials to Observational Studies, Chest 158 (2020) S12–S20. https://doi:10.1016/j.chest.2020.03.010.

[11] Y. Hu, L.S. Wang, Y.P. Jin, S.S. Du, Y.K. Du, X. He, D. Weng, Y. Zhou, Q.H. Li, L. Shen, F. Zhang, Y.L. Su, X.L. Sun, J.J. Ding, W.H. Zhang, H.R. Cai, H.P. Dai, J. H. Dai, H.P. Li, Serum Krebs von den Lungen-6 level as a diagnostic biomarker for interstitial lung disease in Chinese patients, Clin. Respir. J. 11 (2017) 337–345, https://doi.org/10.1111/crj.12341.

[12] I. Nishizono, S. Iida, N. Suzuki, H. Kawada, H. Murakami, Y. Ashihara, M. Okada, Rapid and sensitive chemiluminescent enzyme immunoassay for measuring tumor markers, Clin. Chem. 37 (1991) 1639–1644, https://doi.org/10.1093/clinchem/37.9.1639.

[13] K.B. Brosnihan, M.C. Chappell, Measurement of angiotensin peptides: HPLC-RIA, Methods Mol. Biol. 1527 (2017) 81–99, https://doi.org/10.1007/978-1-4939-6625-7_7.

[14] C.M. Dubois, M.H. Laprise, F. Blanchette, L.E. Gentry, R. Leduc, Processing of transforming growth factor beta 1 precursor by human furin convertase, J. Biol. Chem. 270 (1995) 10618–10624, https://doi.org/10.1074/jbc.270.18.10618.

[15] S. Blackmore, M. Hamilton, A. Lee, M. Worwood, M. Brierley, A. Heath, S. J. Thorpe, Automated immunoassay methods for ferritin: recovery studies to assess traceability to an international standard, Clin. Chem. Lab. Med. 46 (2008) 1450–1457, https://doi.org/10.1515/CCLM.2008.304.

[16] C.P. Price, A.K. Trull, D. Berry, E.G. Gorman, Development and validation of a particle-enhanced turbidimetric immunoassay for C-reactive protein, J. Immunol. Methods 99 (1987) 205–211, https://doi.org/10.1016/0022-1759(87)90129-3.

[17] R. Bais, M. Philcox, Approved recommendation on IFCC methods for the measurement of catalytic concentration of enzymes. Part 8. IFCC Method for Lactate Dehydrogenase (l-Lactate: NAD+Oxidoreductase, EC 1.1.1.27). International Federation of Clinical Chemistry (IFCC), Eur. J. Clin. Chem. Clin. Biochem. 32 (1994) 639–655.

[18] V.M. Ranieri, G.D. Rubenfeld, B.T. Thompson, N.D. Ferguson, E. Caldwell, E. Fan, L. Camporota, A.S. Slutsky, Acute respiratory distress syndrome: The Berlin definition, JAMA 307 (2012) 2526–2533, https://doi.org/10.1001/jama.2012.5669.

[19] D. Chesher, Evaluating assay precision, Clin. Biochem. Rev. 29 (Suppl 1) (2008) S23–S26.

[20] S. André, A.-V. Bruyneel, A. Chirumberro, A. Roman, M. Claus, S. Alard, N. De Vos, M. Bruyneel, Health-Related Quality of Life Improves in Parallel with FEV1 and 6-Minute Walking Distance Test at Between 3 and 12 Months in Critical COVID-19 Survivors, Am. J. Med. Open 100055 (2023) ISSN 2667-0364. Doi: 10.1016/j.ajmo.2023.100055.

[21] L. Truffaut, L. Demey, A.-V. Bruyneel, A. Roman, S. Alard, N. De Vos, M. Bruyneel, Post-discharge critical COVID-19 lung function related to severity of radiologic lung involvement at admission, Respir. Res. 22 (2021) 29, https://doi.org/10.1186/s12931-021-01625-y.

[22] C. Dusart, J. Smet, A. Chirumberro, S. André, A. Roman, M. Claus, A.-V. Bruyneel, O. Menez, S. Alard, N. De Vos, M. Bruyneel, Pulmonary Functional Outcomes at 3 Months in Critical COVID-19 Survivors Hospitalized during the First, Second, and Third Pandemic Waves, J. Clin. Med. 12 (2023) 3712, https://doi.org/10.3390/jcm12113712.

[23] C.S. Calfee, K. Delucchi, P.E. Parsons, B.T. Thompson, L.B. Ware, M.A. Matthay, Subphenotypes in acute respiratory distress syndrome: Latent class analysis of data from two randomised controlled trials, Lancet Respir. Med. 2 (2014) 611–620, https://doi.org/10.1016/S2213-2600(14)70097-9.

[24] C.S. Calfee, K.L. Delucchi, P. Sinha, M.A. Matthay, J. Hackett, M. Shankar-Hari, C. McDowell, J.G. Laffey, C.M. O'Kane, D.F. McAuley, Irish Critical Care Trials Group, Acute respiratory distress syndrome subphenotypes and differential response to simvastatin: secondary analysis of a randomised controlled trial, Lancet Respir. Med. 6 (2018) 691–698, https://doi.org/10.1016/S2213-2600(18)30177-2.

[25] P. Mehta, R.J. Samanta, K. Wick, R.C. Coll, T. Mawhinney, P.G. McAleavey, A. J. Boyle, J. Conlon, M. Shankar-Hari, A. Rogers, C.S. Calfee, M.A. Matthay, C. Summers, R.C. Chambers, D.F. McAuley, C.M. O'Kane, Elevated ferritin, mediated by IL-18 is associated with systemic inflammation and mortality in acute respiratory distress syndrome (ARDS), Thorax 79 (2024) 227–235, https://doi.org/10.1136/thorax-2023-220292.

[26] A.L. Serra, N.J. Meyer, J.R. Beitler, Treatment Mechanism and Inflammatory Subphenotyping in Acute Respiratory Distress Syndrome, Am. J. Respir. Crit. Care Med. 209 (2024) 774–776, https://doi.org/10.1164/rccm.202402-0340ED.

[27] L.D. Bos, L.R. Schouten, L.A. van Vught, M.A. Wiewel, D.S.Y. Ong, O. Cremer, A. Artigas, I. Martin-Loeches, A.J. Hoogendijk, T. van der Poll, J. Horn, N. Juffermans, C.S. Calfee, M.J. Schultz, MARS consortium, Identification and validation of distinct biological phenotypes in patients with acute respiratory distress syndrome by cluster analysis, Thorax 72 (2017) 876–883, https://doi.org/10.1136/thoraxjnl-2016-209719.

[28] P. Luna, M. Fernanda Pérez, J. Castellar-Lopez, A. Chang, Y. Montoya, J. Bustamante, W. Rosales-Rada, E. Mendoza-Torres, Potential of Angiotensin-(1–7) in COVID-19 Treatment, Curr. Protein Pept. Sci. 24 (2022) 89–97, https://doi.org/10.2174/1389203724666221130140416.

[29] C. Yao, T. Parimon, M.S. Espindola, M.S. Hohmann, B. Konda, C.M. Hogaboam, B. R. Stripp, P. Chen, Maladaptive TGF-β Signals to the Alveolar Epithelium Drive Fibrosis after COVID-19 Infection, Am. J. Respir. Crit. Care Med. 208 (2023) 201–204, https://doi.org/10.1164/rccm.202302-0264LE.

[30] Q. Huang, Y. Le, S. Li, Y. Bian, Signaling pathways and potential therapeutic targets in acute respiratory distress syndrome (ARDS), Respir. Res. 25 (2024) 30, https://doi.org/10.1186/s12931-024-02678-5.

[31] S. Mandal, J. Barnett, S.E. Brill, J.S. Brown, E.K. Denneny, S.S. Hare, M. Heightman, T.E. Hillman, J. Jacob, H.C. Jarvis, M.C.I. Lipman, S.B. Naidu, A. Nair, J.C. Porter, G.S. Tomlinson, J.R. Hurst, ARC Study Group, 'Long-COVID': a cross-sectional study of persisting symptoms, biomarker and imaging abnormalities following hospitalisation for COVID-19, Thorax 76 (2021) 396–398, https://doi.org/10.1136/thoraxjnl-2020-215818.

[32] N. De Vos, C. Duterme, Z. Ouanani, D. Dirickx, M. Bruyneel, A. Roman, S. Alard, F. Ponthieux, M. Lauwers, E. Mathieu, C. Goudji, S. André, D. Barglazan, C. Dusart, L. Truffaut, F. Cotton, Follow-up of novel KL-6 and routine biomarkers in covid-19 survivors 1 year post-ICU, Clin. Chem. Lab. Med. 59 (s1) (2021) s94–s119.

[33] N. De Vos, M. Bruyneel, C. Duterme, A. Roman, H. Dahma, S. Alard, S. André, D. Barglazan, A. Chirumberro, F. Cotton, A-249 Theranostic Algorithm: sensitivity and Specificity of a Composite Index Test for Guiding Treatment in Severe COVID-19, Clin. Chem. 69 (2023) s1:hvad097.220. Doi: 10.1093/clinchem/hvad097.220.

[34] D.H. Peng, Y. Luo, L.J. Huang, F.L. Liao, Y.Y. Liu, P. Tang, H.N. Hu, W. Chen, Correlation of Krebs von den Lungen-6 and fibronectin with pulmonary fibrosis in coronavirus disease,, Clin. Chim. Acta 517 (2021) (2019) 48–53, https://doi.org/10.1016/j.cca.2021.02.012.

[35] D. Kızılırmak, S. Sarı, F. Can, Y. Havlucu, Radiological findings based comparison of functional status in patients who have post-covid lung injury or idiopathic pulmonary fibrosis, BMC Pulm. Med. 23 (2023) 234, https://doi.org/10.1186/s12890-023-02527-z.

[36] M. Bruyneel, A. Chirumberro, S. Andre, A. Roman, M. Claus, A.-V. Bruyneel, S. Alard, F. Cotton, N. De Vos, Correlation of clinical, radiological outcomes and novel KL-6 biomarker levels in COVID-19 survivors one year post-ICU, Eur. Respir. J. 62 (2023) s67:PA286. Doi: 10.1183/13993003.congress-2023.pa286.

[37] E. Anastasi, L. Manganaro, E. Guiducci, S. Ciaglia, M. Dolciami, A. Spagnoli, F. Alessandri, A. Angeloni, A. Vestri, C. Catalano, P. Ricci, Association of serum Krebs von den Lungen-6 and chest CT as potential prognostic factors in severe acute respiratory syndrome SARS-CoV-2: a preliminary experience, Radiol. Med. 127 (2022) 725–732. https://doi:10.1007/s11547-022-01504-6.

[38] A.J. Podolanczuk, C.C. Thomson, M. Remy-Jardin, L. Richeldi, F.J. Martinez, M. Kolb, G. Raghu, Idiopathic pulmonary fibrosis: state of the art for 2023, Eur. Respir. J. 61 (2023) 2200957, https://doi.org/10.1183/13993003.00957-2022.

[39] E. Poggiali, D. Zaino, P. Immovilli, L. Rovero, G. Losi, A. Dacrema, M. Nuccetelli, G. B. Vadacca, D. Guidetti, A. Vercelli, A. Magnacavallo, S. Bernardini, C. Terracciano, Lactate dehydrogenase and C-reactive protein as predictors of respiratory failure in CoVID-19 patients, Clin. Chim. Acta 509 (2020) 135–138, https://doi.org/10.1016/j.cca.2020.06.012.

[40] J.R. Delanghe, M.M. Speeckaert, M.L. De Buyzere, The host's angiotensin-converting enzyme polymorphism may explain epidemiological findings in COVID-19 infections, Clin. Chim. Acta 505 (2020) 192–193, https://doi.org/10.1016/j.cca.2020.03.031.

[41] A.W. Azagew, Z.W. Beko, Y.M. Ferede, H.S. Mekonnen, H.K. Abate, C. K. Mekonnen, Global prevalence of COVID-19-induced acute respiratory distress syndrome: systematic review and meta-analysis, Syst. Rev. 12 (2023) 212, https://doi.org/10.1186/s13643-023-02377-0.

[42] H. Hatabu, K.M. Kaye, D.C. Christiani, Viral Infection, Pulmonary Fibrosis, and Long COVID, Am. J. Respir. Crit. Care Med. 207 (2023) 647–649, https://doi.org/10.1164/rccm.202211-2121ED.

[43] C.F. McGroder, M.M. Salvatore, B.M. D'Souza, E.A. Hoffman, M.R. Baldwin, C. K. Garcia, Improved pulmonary function and exercise tolerance despite persistent pulmonary fibrosis over 1 year after severe COVID-19 infection, Thorax 79 (2024) 472–475, https://doi.org/10.1136/thorax-2023-220370.

[44] S. Soliman, H. Soliman, M. Crézé, P.Y. Brillet, D. Montani, L. Savale, X. Jais, S. Bulifon, E.M. Jutant, E. Rius, M. Devilder, A. Beurnier, R. Colle, M. Gasnier, T. Pham, L. Morin, N. Noel, A.L. Lecoq, L. Becquemont, S. Figueiredo, A. Harrois, M.-F. Bellin, X. Monnet, O. Meyrignac, COMEBAC study group, Radiological pulmonary sequelae after COVID-19 and correlation with clinical and functional pulmonary evaluation: results of a prospective cohort, Eur. Radiol. 34 (2024) 1037–1052, https://doi.org/10.1007/s00330-023-10044-0.

[45] S. Wallemacq, C. Danwang, A. Scohy, L. Belkhir, J. De Greef, B. Kabamba, J. C. Yombi, A comparative analysis of the outcomes of patients with influenza or COVID-19 in a tertiary hospital in Belgium, J. Infect. Chemother. 28 (2022) 1489–1493, https://doi.org/10.1016/j.jiac.2022.07.012.

[46] C.Y. Yang, C.S. Chen, G.T. Yiang, Y.L. Cheng, S.B. Yong, M.Y. Wu, C.J. Li, New Insights into the Immune Molecular Regulation of the Pathogenesis of Acute Respiratory Distress Syndrome, Int. J. Mol. Sci. 19 (2018) 588, https://doi.org/10.3390/ijms19020588.

[47] L. Zamai, The Yin and Yang of ACE/ACE2 Pathways: The Rationale for the Use of Renin-Angiotensin System Inhibitors in COVID-19 Patients, Cells 9 (2020) 1704, https://doi.org/10.3390/cells9071704.

[48] S.J. Forrester, G.W. Booz, C.D. Sigmund, T.M. Coffman, T. Kawai, V. Rizzo, R. Scalia, S. Eguchi, Angiotensin II Signal Transduction: An Update on Mechanisms of Physiology and Pathophysiology, Physiol. Rev. 98 (2018) 1627–1738, https://doi.org/10.1152/physrev.00038.2017.

[49] H.H. Hu, D.Q. Chen, Y.N. Wang, Y. Feng, G. Cao, N.D. Vaziri, Y.Y. Zhao, New insights into TGF-β/Smad signaling in tissue fibrosis, Chem. Biol. Interact. 292 (2018) 76–83, https://doi.org/10.1016/j.cbi.2018.07.008.

[50] M.W. Millar, F. Fazal, A. Rahman, Therapeutic Targeting of NF-κB in Acute Lung Injury: A Double-Edged Sword, Cells 11 (2022) 3317, https://doi.org/10.3390/cells11203317.

[51] Y. Meng, C.H. Yu, W. Li, T. Li, W. Luo, S. Huang, P.S. Wu, S.X. Cai, X. Li, Angiotensin-converting enzyme 2/angiotensin-(1–7)/Mas axis protects against lung fibrosis by inhibiting the MAPK/NF-κB pathway, Am. J. Respir. Cell Mol. Boil. 50 (2014) 723–736, https://doi.org/10.1165/rcmb.2012-0451OC.

[52] O. Piazza, G. Scarpati, G. Boccia, M. Boffardi, P. Pagliano, KL-6 in ARDS and COVID-19 Patients, Transl. Med. Unisa. 24 (2022) 12–15. https://doi:10.37825/2239-9754.1035.

[53] Y. Meng, T. Li, G.S. Zhou, Y. Chen, C.H. Yu, M.X. Pang, W. Li, Y. Li, W.Y. Zhang, X. Li, The angiotensin-converting enzyme 2/angiotensin (1–7)/Mas axis protects against lung fibroblast migration and lung fibrosis by inhibiting the NOX4-derived ROS-mediated RhoA/Rho kinase pathway, Antioxid. Redox Signal. 22 (2015) 241–258, https://doi.org/10.1089/ars.2013.5818.

[54] B.M. Henry, J.L. Benoit, B.A. Berger, C. Pulvino, C.J. Lavie, G. Lippi, S.W. Benoit, Coronavirus disease,, is associated with low circulating plasma levels of angiotensin 1 and angiotensin 1,7, J. Med. Virol. 93 (2021) (2019) 678–680, https://doi.org/10.1002/jmv.26479.

[55] A.L. Valle Martins, F.A. da Silva, L. Bolais-Ramos, G.C. de Oliveira, R.C. Ribeiro, D. A.A. Pereira, F. Annoni, M.M.L. Diniz, T.G.F. Silva, B. Zivianni, A.C. Cardoso, J. C. Martins, D. Motta-Santos, M.J. Campagnole-Santos, F.S. Taccone, T. Verano-Braga, R.A.S. Santos, Increased circulating levels of angiotensin-(1–7) in severely ill COVID-19 patients, ERJ Open Res. 7 (2021) 00114–02021, https://doi.org/10.1183/23120541.00114-2021.